Short Communication: A database of the global distribution of (U-Th)/He ages and U, Th contents of goethites

Hevelyn S. Monteiro[1*], Kenneth A. Farley[1], Paulo M. Vasconcelos[2]

1. California Institute of Technology, Pasadena, CA, 91125, USA

2. The University of Queensland, Brisbane, QLD,4072, Australia

Correspondence to: hevevelynbr@gmail.com

Abstract. Terrestrial supergene goethites of known ages record information on changes in weathering conditions through time. Here we present a database of (U-Th)/He ages and U and Th contents of goethites from different weathering environments around the globe. By consolidating published data collected at four different laboratories and unpublished data collected at the Noble Gas Laboratory at Caltech, we aim to give an overview of the work carried out by geochronologists and geochemists in the last 20 years. The database contains 2609 (U-Th)/He ages of goethites from 10 countries; most of the ages come from Brazil and Australia.

1. Introduction

Supergene goethite (α-FeOOH) is the most thermodynamically stable and abundant iron oxyhydroxide in weathering environments (Sposito, 1998) (technical terms and definitions are listed in the Glossary - https://github.com/hevelyn-monteiro/GlobalGoethite_U-Th-He_Ages.git). Goethite precipitates under oxidizing, acid, neutral, or basic conditions when weathering solutions interact with Fe-rich rocks, sediments, and soils at temperatures ranging from ~ 5 to ~ 60° C (Yapp, 2001). In natural environments, the coexistence of supergene goethite with other iron oxides and oxyhydroxides such as hematite (α-Fe$_2$O$_3$), maghemite (γ-Fe$_2$O$_3$), lepidocrocite (γ-FeOOH), and akageneite (β-FeOOH), along with changes in its chemical composition due to the incorporation of metal cations (e.g., Al^{3+}, Mn^{4+}, Cu^{+2}), indicates complex patterns of mineral precipitation that reflect changes in environmental conditions across time and space. For instance, weathering profile moisture deficiency leads to co-existence of goethite and hematite (e.g., Heller et al., 2022), suggesting either the dehydration of goethite to hematite under extended periods of dry-hot conditions, or alternate precipitation of goethite-hematite when conditions change from wet to dry. Due to its widespread distribution and uniquely supergene origin, goethite is a preferred mineral for dating weathering processes; hematite, common in weathering profiles as either supergene or hypogene minerals, typically plays a secondary role. Therefore, by determining the ages of supergene goethites present in weathering profiles we can trace major changes in Earth's climatic and tectonic histories.

As goethite records information on water-rock interactions in near surface environments (e.g., Yapp, 2001), it potentially reveals how old weathering profiles are, how weathering solutions evolved through time, and how fast or slow chemical weathering and denudation transform rocks at the surface and in the shallow subsurface. Attempts to date supergene goethite date back to Strutt (1910). Lippolt et al. (1998) revisited the (U-Th)/He method to determine the ages and evaluate He retentivity in supergene goethites. Shuster et al. (2005) used the ^{4}He/^{3}He method to quantify He retentivity in various types of goethites, showing that (U-Th)/He results could be corrected for He losses and that well-crystallized goethite retained more than 90% of its He for millions of years. Farley et al. (2024) showed that ^{4}He/^{3}He incremental heating profiles help to differentiate He-retentive from non-retentive goethite, but it does not permit calculating He diffusivity parameters (activation energy and frequency factor) for goethite because experimental He release occurs during phase transformation. Mostly due to our improved understanding of how to date and assess the reliability of the results, the combined (U-Th)/He-^{4}He/^{3}He method has been successfully used to date goethites from lateritic profiles in Brazil, Australia, and China (Shuster et al., 2005; Vasconcelos et al., 2013; Deng et al., 2017) and from paleosols in Switzerland (Hoffman et al., 2017). Based on a better understanding of which types of goethite yield reliable geochronological results, numerous studies have used (U-Th)/He geochronology of goethite from various settings to obtain reliable age information and shed light on changes in global environmental conditions.

The application of (U-Th)/He dating to goethite-bearing weathering profiles across the globe has provided new insights into the Earth's surficial history. Studies in Western Australia (e.g., Heim et al., 2006; Vasconcelos et al., 2013; Danisik et al., 2013; Yapp and Shuster, 2017) and Brazil (e.g., Lima, 2008; Monteiro et al., 2014, 2018(a,b), 2022; Conceição et al., 2024) have unveiled a protracted weathering history, showing that goethite age distribution depends on climate and erosional history. Similarly, studies in French Guiana (Heller et al., 2022), Suriname (Ansart et al., 2022), Morocco (Verhaert et al., 2022), and Tunisia (Yans et al., 2021) confirm the influence of paleoclimate and landscape evolution on weathering and supergene ore genesis. Dated pisoliths from the Bohnerz Fomation paleosol in Central Europe (Hofmann et al., 2017) show intensification of weathering and soil formation during the Miocene. These studies, and many others compiled here, highlight the utility and applicability of goethite (U-Th)/He geochronology. Also importantly, (U-Th)/He geochronology of goethite confirmed independent weathering history information obtained from manganese oxide ^{40}Ar/^{39}Ar geochronology (Vasconcelos et al., 2015; Riffel et al., 2015).

Here we compile a global database of goethite distribution, (U-Th)/He ages, and U and Th concentrations, the latter a byproduct of the age determination. From this global compilation we infer the main factors controlling the formation and preservation of supergene goethite. Building upon the findings from each individual study, we aim to assess the influence of environmental conditions on changes in the frequency of precipitation and preservation of goethites in weathering profiles.

2. Goethite U-Th-He database

The database (https://github.com/hevelyn-monteiro/GlobalGoethite_U-Th-He_Ages.git) comprises 2609 goethite (U-Th)/He ages, with 2359 U (ppm) and 2355 Th (ppm) measurements. Most of these ages – 2187 – come from published studies, while the remaining are our unpublished measurements made at Caltech over the last two decades using methods described in Shuster et al. (2005) and Monteiro et al. (2014, 2018a). Some authors report U and Th measurements in units such as ng, nmol, or nmol/g. For cases where the mass of the analyzed grain was not provided and parent element amounts are reported, it was impossible to calculate concentrations in ppm. Consequently, only the ages of these samples are summarized here. In addition to U and Th concentrations and (U-Th)/He ages, the database also contains information on geographical location, elevation (m), sample depth (m), bedrock, Sm (ppm) and eU (ppm) concentrations, and Th/U values. Effective uranium (eU) is defined as (U + 0.235 Th) and is a single metric that approximates the alpha particle production rate.

Note that many entries in the database represent analyses of goethite subsamples from a single hand sample. In some cases, these may represent replicates of a single generation of goethite, while in others they may represent distinct generations. In the discussion below we make no attempt to weigh results for possible duplicate analyses; every analysis is considered an independent result.

Figure 1 illustrates the map distribution of (U-Th)/He dated goethites. Most samples are from Brazil [1428] and Australia [486]. This dominance reflects the interests of the researchers driving the studies, the abundance of supergene goethite in lateritic profiles and ferricretes in the two countries, and the ease of access to sampling sites in open-pit mining operations. The two countries are major iron ore producers, and it makes sense to search for iron minerals in these locations. In addition, Brazil and Australia sit at similar geographic positions near the tropics but contrast greatly in present and paleo climates and Cenozoic plate motion paths, providing excellent test grounds for assessing the relative roles of climate and tectonics on the formation and preservation of goethites in the landscape. (U-Th)/He ages for goethites are also available from Switzerland [195], Suriname [193], French Guiana [134], Morocco [55], China [52], USA [41], Tunisia [14], and Canada [6]. Goethites from different environments provide information on geological processes of local and global significance. Therefore, we will summarize the most important characteristics of each type of weathering environment from which ages of goethites have been obtained so far, along with the different types of goethites investigated by (U-Th)/He geochronology.
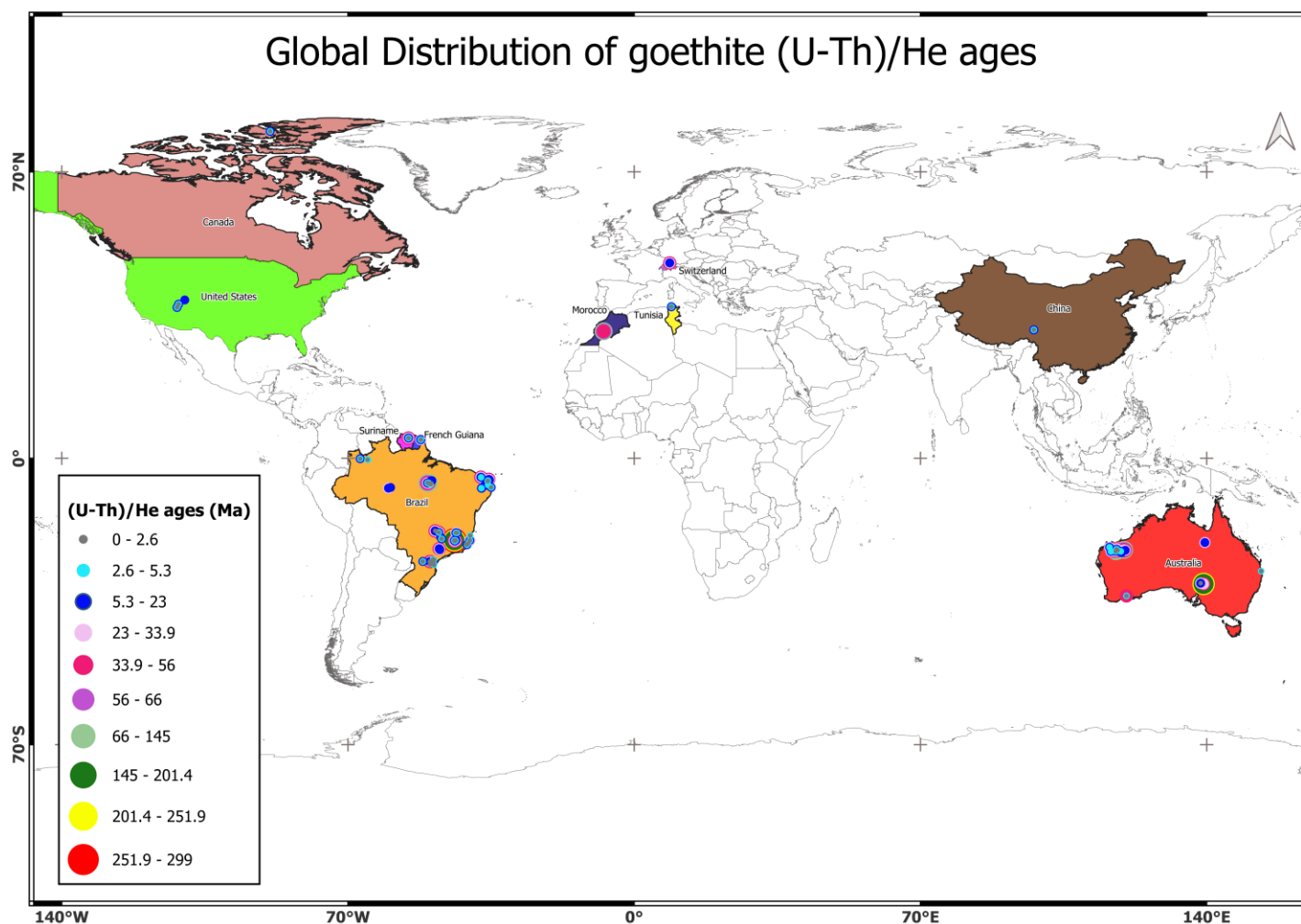
Figure 1 illustrates the geographical distribution of dated goethites worldwide. The country colors were selected to align with the histogram colors in Figure 5. A total of 2609 (U-Th)/He ages were compiled from published and unpublished research. The large majority of dated goethites come from Brazil (55%) and Australia (18%). Globally, the largest number of goethites are of Miocene age (40%), while the second (20%) and third (16%) largest groups of dated goethites fall within the Pleistocene and Pliocene epochs, respectively. (U-Th)/He ages older than 65 Ma only occur in Brazil (Amazon and Quadrilátero Ferrífero), Australia (Hamersley Province and Flinders Ranges), and Morocco.

3. Weathering Environments and Types of Goethite

Table 1 (https://github.com/hevelyn-monteiro/GlobalGoethite_U-Th-He_Ages.git) summarizes relevant information about weathering environments hosting goethite-bearing profiles included in our (U-Th)/He geochronology compilation. Goethite (U-Th)/He ages are available for nine distinct weathering environments: lateritized banded iron formation (BIF); channel iron deposit; nickel laterite; lateritized alkaline-carbonatite complex; lateritized igneous rocks; lateritized continental

sediments; karsts; and coal deposits. These environments differ in bedrock composition, landscape settings, erosion and burial histories, and weathering ages (Table 1). Below we present a summary of the main types and the distribution patterns of goethites in these environments.

In tropical environments, lateritized banded iron formations (BIFs) are capped by a canga layer that consists of well-crystallized goethite cementing loose fragments of weathered BIF or replacing primary minerals. Goethite occurs in diverse aggregate forms, including botryoidal or colloform masses, massive cements (Fig. 2a), pore-filling films and coatings (Fig.2b), pisolithic structures, and biogenic textures (Monteiro et al., 2014). Goethite in canga may be contaminated with primary minerals such as hematite and magnetite that have survived weathering (Fig. 3d). However, recurrent iron dissolution-reprecipitation processes efficiently purify supergene goethite cements in BIFs (Fig. 3a), and samples often yield tightly clustered ages (e.g., Monteiro et al., 2014, 2018a). In some cases, however, recurrent iron dissolution-reprecipitation produces multiple goethite generations in a sample, which requires the analysis of several sub-aliquots from the same sample to unravel its complete history of mineral precipitation (Monteiro et al., 2020). Below the canga horizon, lateritized BIFs host deep hematite saprolites. In these saprolites, there are veins of supergene goethite often replacing carbonate veins (Fig. 2a). Goethites from these settings are pure, often display biogenic textures (Levett et al., 2020a, b), and they are ideal for geochronology.

In the lateritized channel iron deposits (CIDs) of Western Australia, pisolithic goethite firmly bound by goethite cements produce a wealth of samples for analysis (Heim et al., 2006; Denišik et al., 2013). In addition, ferruginized clays and wood fragments (Fig. 2c) offer additional phases for geochronology. Pisolithic goethite often exhibit partial mineral replacement and the presence of detrital hematite cores that must be separated and independently dated (Denišik et al., 2013).

In gossans and lateritized Cu-Au deposits, goethite forms large, pure, well-crystallized colloform masses (Fig. 2d) (Monteiro et al., 2018a). It fills voids created by weathering of massive sulfides. The duricrust overlying gossans host recrystallized gossan fragments that exhibit complex textures, where Al-rich and Al-poor goethite (Fig. 3c) coexist, together with gibbsite, hematite, anatase, and clay minerals.

In nickel laterites, goethite is present throughout the weathering profile, but goethite suitable for geochronology is most concentrated above the limonite zone, where the finely crystalline goethite produced by the incongruent dissolution of olivines and pyroxenes undergoes recurrent dissolution-reprecipitation, forming authigenic colloform vitreous goethite. These goethite masses are generally pure, but they may contain primary chromite grains as contaminants. In these systems, the fine crystalline goethite – limonite – is not He retentive, and only the crystalline colloform masses (Fig. 2e) produced late in the history of weathering are suitable for geochronology. This may bias the results towards younger weathering ages.

Lateritized alkaline-carbonatite complexes contain a complex assemblage of rock types (e.g., phoscorite, carbonatite, syenites) and often host sulfide mineralization. Most crystalline goethite in weathered carbonatites is either derived from weathering of sulfides or olivine-pyroxene-magnetite precursors. Commonly, goethites are visually pure and massive, and

may contain significant concentrations of dopants, such as aluminum. Small inclusions of monazite, ilmenite, or magnetite may pose problems to geochronology (Conceição et al., 2022).

Deeply weathered basalts host significant concentrations of goethite, either in duricrusts and pisolithic horizons near the surface or as Fe-metasomatized horizons or veins in the basalts (Fig. 2f) (Riffel et al., 2016). Goethite is rich in Al, Ti, Ni, and other trace elements and may host relic grains of ilmenite or supergene rutile. Goethite may range from well to poorly crystallized, which will impact on the reliability of the geochronological results (Farley et al., 2024). Similarly, duricrusts developed on granites and intermediate igneous rocks contain both well crystallized homogeneous goethites and heterogeneous goethites intergrown with hematite, gibbsite, Ti-oxides, and kaolinite. Goethite aggregates vary from botryoidal to massive to pisolithic structures embedded in orange-ochre or red matrix (Heller et al., 2022).

In weathered continental sediments, goethite occurs both as transported duricrust fragments and pisoliths, or as in situ cements coating concretions, replacing tree roots, or forming concentric accretionary masses forming authigenic pisoliths (Fig 2g) (Lima, 2008; Monteiro et al., 2022). Many of the continental sediments investigated by goethite geochronology contain abundant detrital Th-rich minerals (xenotime, monazite, thorite, etc.). Goethite in these sediments commonly coexists with kaolinite, quartz, hematite, ilmenite, rutile, and many of the Th-bearing phases identified above. Pisolithic goethites in these settings are often well crystallized and devoid of contaminants (Fig 3e) (e.g., Monteiro et al., 2022).

In the dolomite karst environments of Morocco, centimeter-thick masses of pure botryoidal goethite precipitated from mixing of iron-rich, oxygen-poor solutions with oxygenated meteoric waters (Verhaert et al., 2022). The purity of those goethites makes them ideal samples for (U-Th)/He geochronology. In Brazil, karst formation on resistant quartzite exposed lenses of hematite-phyllite to pervasive lateritic weathering, resulting in deeply weathered lateritic profiles (de Campos et al., 2023). Repeated cycles of goethite dissolution and reprecipitation lead to the formation of duricrusts composed of a complex mixture Al-rich goethite, gibbsite, hematite, Ti-oxides, and quartz (de Campos et al., 2023).

In coal deposits, goethite cementation of tree logs (Fig. 2h) aids in the complete preservation of tree trunks before burial and coalification, including their organic macro features and cell structures. These well crystallized goethites may coexist with late-stage hematite and pyrite formed after burial (Fig. 3f). (U-Th)-He ages obtained for these goethites probably represent cooling ages associated with exhumation of the coal deposits.
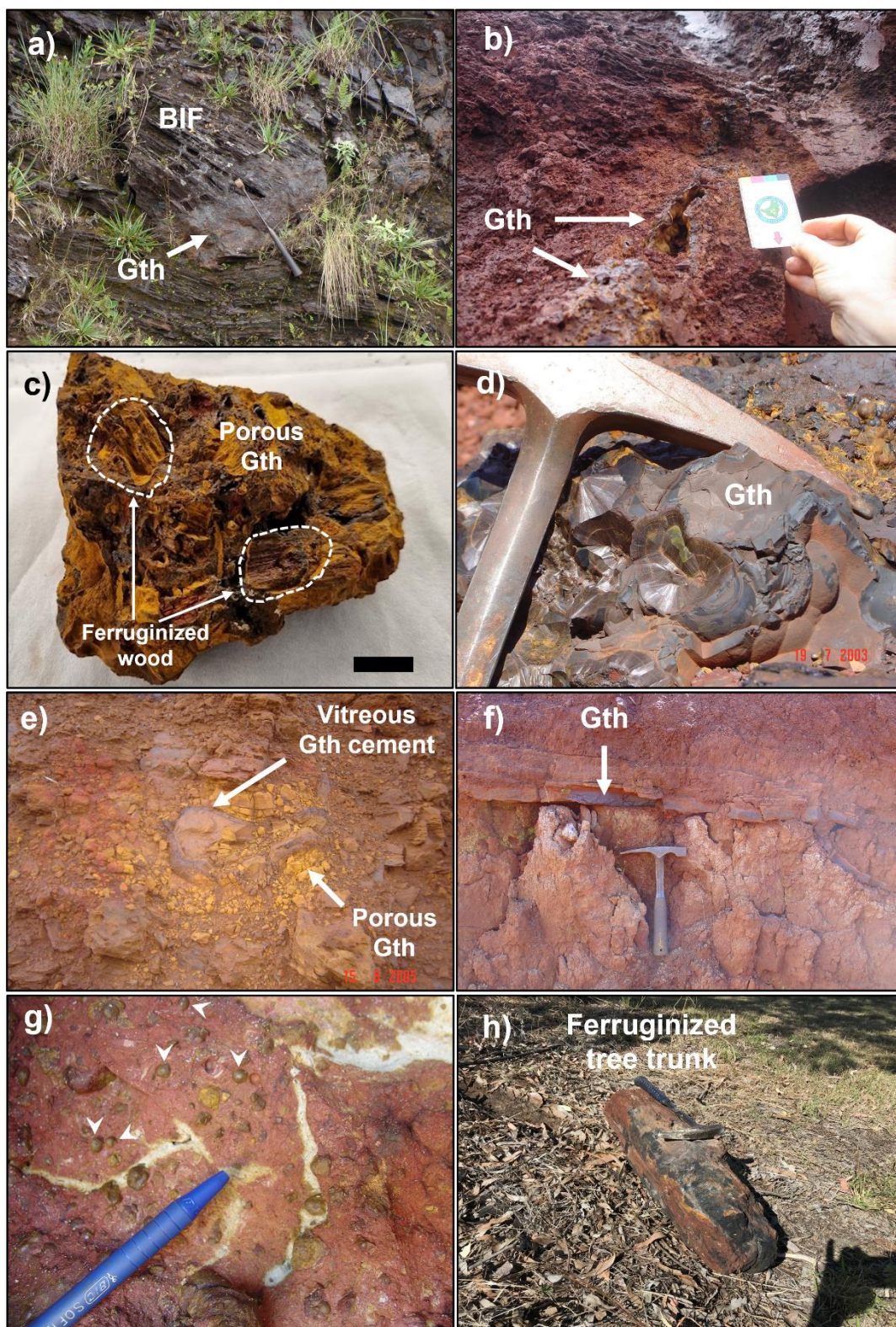
Figure 2. Goethite occurrences in different weathering environments: a) massive goethite substituting carbonates or sulfides in BIF; b) cavity-filling goethite in duricrust (canga); c) yellow goethite replacing fragments of wood and sediments from CID; d)

botryoidal pure goethite from large cavities in Cu-Au deposit; e) massive goethite at the soil-saprolite boundary from weathered basalts; f) pisolithic goethites (arrows) and concretions from lateritized continental sediments; and g) tree log replaced by goethites.
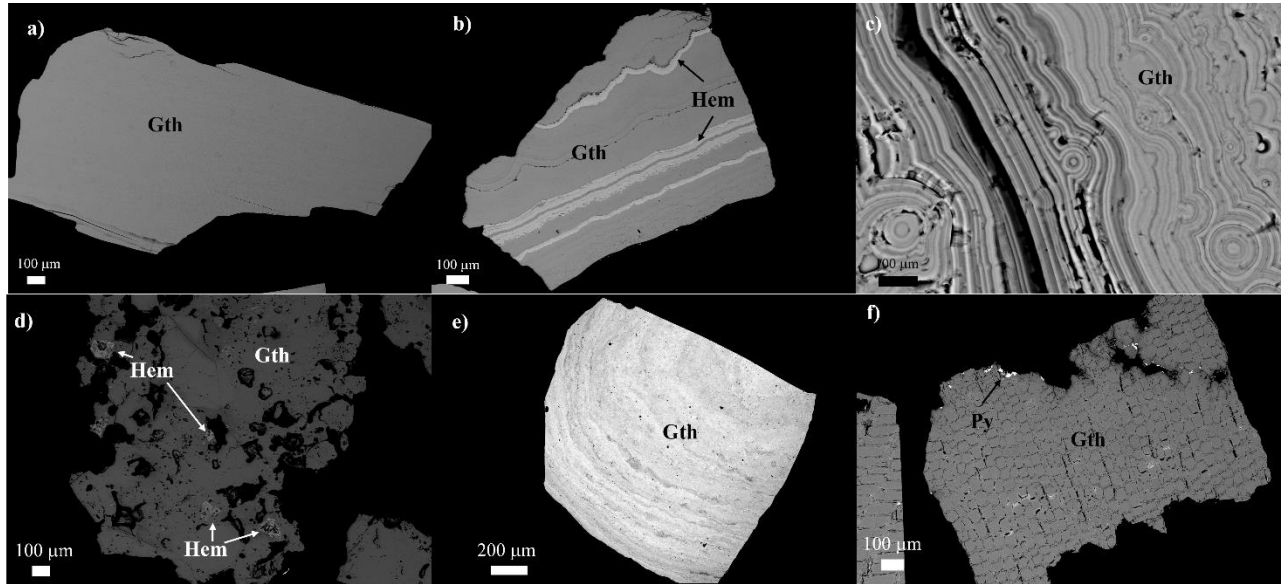
Figure 3. Micrographs of typical grains used in geochronology: a) pure goethite; b) alternate layers of pure goethite and hematite; c) alternate layers of goethite of different chemical composition; d) porous goethite grain containing relic hypogene hematite inclusions; e) pisolithic goethite; and f) a fragment of fossilized tree trunk showing cells replaced by goethite.

4. U and Th concentrations in globally distributed goethites

Uranium and thorium behave differently under earth's surface conditions. U^{4+}, $U(V)O_2^+$, and $U(VI)O_2^{2+}$ are commonly complexed in surface waters (Langmuir, 1978). The stability of different uranium complexes in weathering solutions depends on the oxidation potential and pH of the fluid, the amount of dissolved oxygen, the presence of sorptive agents, and the concentration of other species such as F^-, Cl^-, CO_3^{2-}, SO_4^{2-}, PO_4^{3-}, OH^-, O^{2-}, and organic complexing ligands (Langmuir, 1978). Uranium is relatively mobile in oxidizing solutions, but U^{4+} concentrations in weathering solutions are low because U tends to precipitate as insoluble uraninite (UO_2) and coffinite ($U(SiO_4).nH_2O$) when solutions interact with organic matter (Langmuir, 1978). Massey et al. (2014) show that incorporation of U into the goethite structure may occur via reduction of U(VI) to U(V) in the presence of Fe^{2+} in solution during ferrihydrite transformation to goethite. The prerequisite of an unstable precursor to goethite still needs confirmation. Reduction of $U(VI)O_2^{2+}$ to UO_2 and adsorption of $U(VI)O_2^{2+}$ on the goethite surface are other retention pathways (Massey et al., 2014). In contrast, Th^{4+} complexes are much less mobile and tend to remain very close to their mineral sources. However, organic complexes of Th can be stable between

pHs 4 and 8 (Boyle, 1982), increasing Th mobility in certain surficial environments (Monteiro et al., 2014, 2018; de Campos et al., 2022).

Uranium and thorium concentrations in goethites can vary significantly within a weathering profile, and even within a single hand-sample. Variations in goethite U- and Th-contents are associated with changes in the composition of the source rocks, local geochemical conditions, goethite precipitation mechanism, and the possible presence of microscopic inclusions (e.g., monazite) within the goethite grain selected for analysis. Commonly, goethites enriched in U are depleted in Th and vice-versa. However, goethites from some weathering environments may record active mobilization of both elements through time. For instance, de Campos et al. (2023) demonstrates that recurrent infiltration of organic acid-rich solutions into hematite-phyllite layers intercalated with quartzites promoted the dissolution-reprecipitation of goethites and recycling of U and Th in these restricted environments.

Figure 4 illustrates the concentrations of U and Th in goethites from various weathering environments worldwide. The protracted leaching process within long-lived duricrusts enriches surface goethites in Al and Th. This feature is particularly evident in samples from lateritized BIFs (Fig. 4e). Goethites from duricrusts on lateritized igneous rocks (Fig. 4d) show similar enrichment. On the other hand, there is an apparent co-enrichment in U and Th in CID goethites (Fig. 4b; results from only one CID sample). Colloform goethites from weathered massive sulfide deposits often contain hundreds to thousands of ppm U but very little Th (Fig. 4a). Similarly to cangas, duricrusts blanketing massive sulfide deposits also contain goethites enriched in Th (Monteiro et al., 2018a). Commonly, goethites contain less than 50 ppm U, except for those from weathered IOCG deposits, lateritized alkaline-carbonatite complexes (ACC) and some continental sediments (Fig. 4a, c, g). Most goethites from lateritized ACC plot within one of two distinct groups (U-rich/Th-poor or U-poor/Th-rich); a few goethites plot in-between (Fig. 4c). Goethites from quartzite karsts (Fig. 4f) consistently show higher concentrations of Th, while dolostone karst shows the opposite trend (high U). Lateritized continental sediments (Fig. 4g) contain the highest Th contents of all goethites (up to ~765 ppm). These high Th contents reveal the presence of detrital Th minerals (e.g., monazite or thorite) in the sedimentary units and attest to the conservative behavior of Th with respect to U during in situ weathering (partial or complete dissolution) of detrital phases. An extreme example of U- and Th-poor goethite is the fossilized tree trunk from the Springsure Coal deposit (Fig. 4i), Queensland, which shows concentrations ≤ 0.8 ppm.
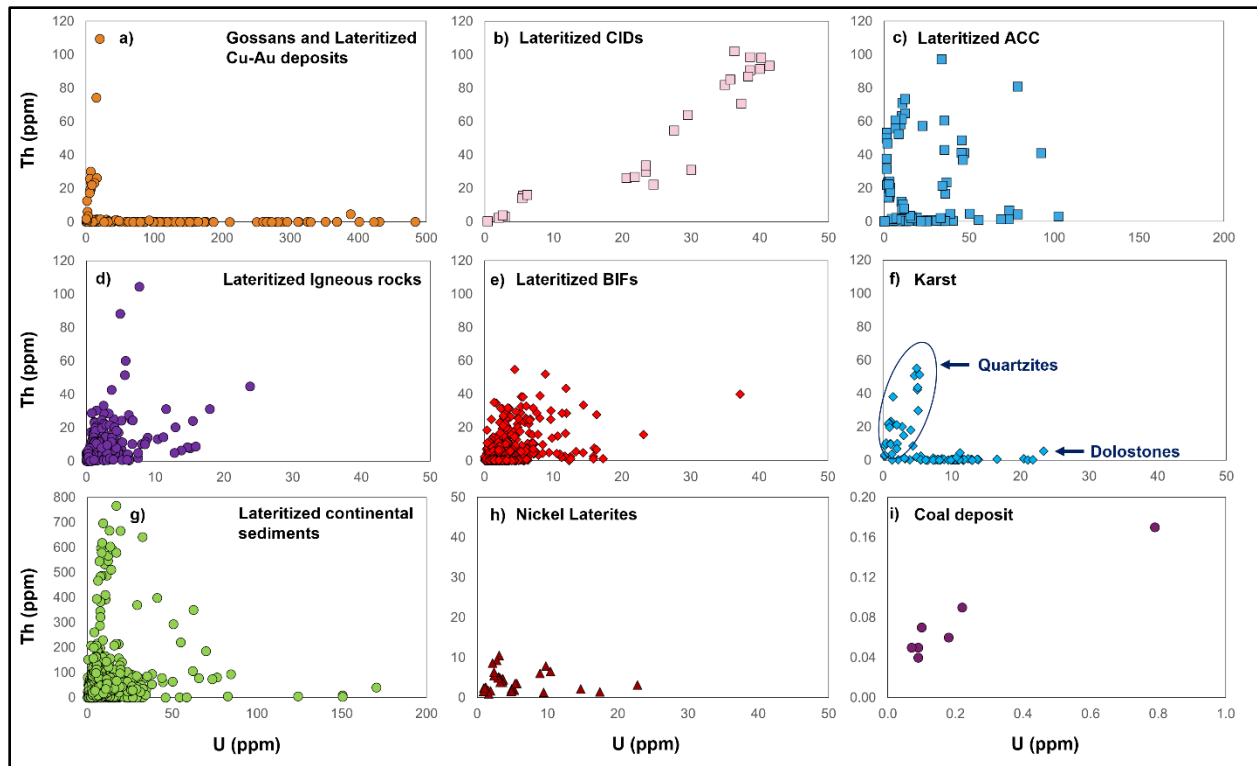
Figure 4. Uranium and Th concentrations of goethites from nine distinct weathering environments.

5. The global distribution of goethite (U-Th)/He ages

Figure 5 illustrates histograms of the distribution of goethite (U-Th)/He ages from 100 to < 1 Ma for ten localities across the globe. A quick comparison of Figures 1 and 5 reveal that only cratonic South America and Australia have been studied with sufficient coverage – in areal distribution, diversity of geological environments, and number of sites and samples analyzed – to permit a continental-scale interpretation of their weathering histories. All other continents have been targeted at local scales, providing useful insights into weathering histories at these sites but impeding broader interpretations. The other significant finding from the compilation is that sites that were weathered and subsequently buried – e.g., Morocco and Switzerland, Figure 5 – preserve a snapshot of the weathering histories at those sites prior to burial. Burial and protection from subsequent surficial processes preserve that ancient history but preclude information on more recent post-burial processes. In contrast, sites that formed at the earth's surface in remote times but continued exposed to surficial processes uninterruptedly – e.g., Brazil, Australia, Suriname, Guiana, Figure 5 – have undergone significant re-setting of the ancient history by more-recent mineral dissolution-reprecipitation. These sites provide an integrated history of weathering in which the most ancient processes become progressively erased by more recent water-rock interaction. The limited number of sites and samples studied for North America (Canada and the USA) and China make their weathering histories incomplete. A noticeable aspect is that the sites targeted so far appear to only host young weathering phases. Targeting sites in landscape

positions and geological environments more likely to host a more complete integrated weathering history would improve our understanding of how these continents responded to changing tectonics and climate throughout the Cenozoic.
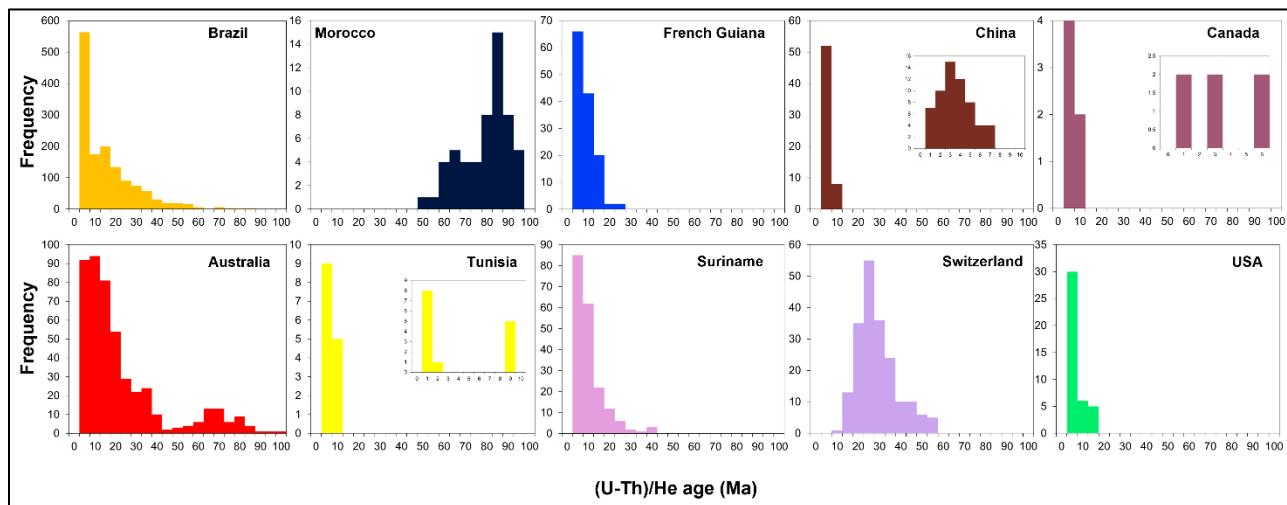
Figure 5. Histograms representing the distribution of goethite (U-Th)/He ages across various regions globally. The histograms offer a detailed insight into the age distribution patterns within each region. Peaks or clusters in the histograms indicate predominant age ranges, while the spread or dispersion of data points provides information on the variability of ages within each region. By combining geographical information with age distribution data, global trends and spatial variations in goethite (U-Th)/He ages show that geological processes and environmental factors influencing the formation and evolution of goethite-bearing weathering profiles differ across the planet.

Another important aspect of our global compilation of (U-Th)/He ages for goethites (Figure 6) is the absence of correlation between (U-Th)/He age (Ma) *vs* eU (ppm). Effective uranium is commonly used as a proxy for radiation damage in a mineral (Flowers et al., 2007). As previously documented for apatite, radiation damage may increase He retentivity in minerals (Flowers et al., 2007). If He loss in nature is important, and if radiation damage makes goethites more retentive, a positive correlation between age and eU should be expected (Bassal et al., 2022). No such correlation is observed for the global database of goethite ages, suggesting that radiation damage is not a significant factor controlling He retentivity in goethite.
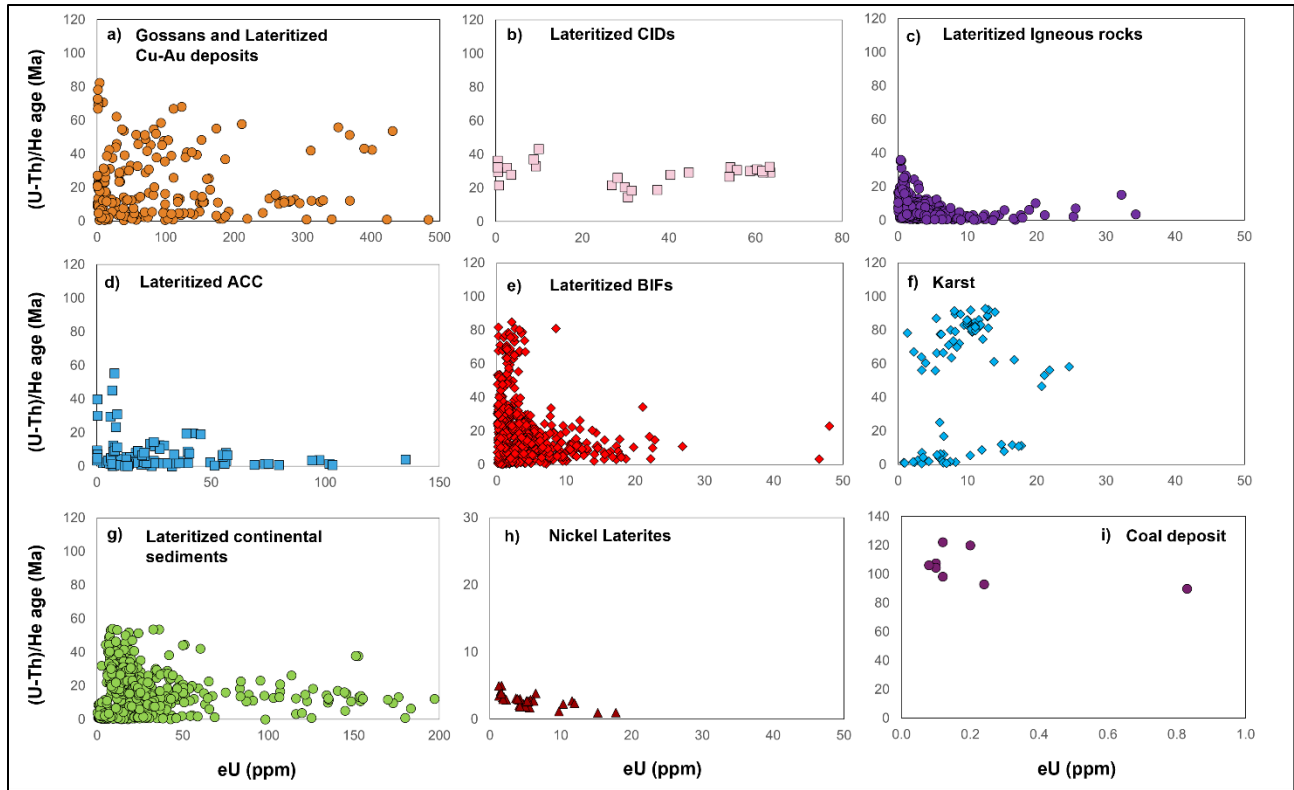
Figure 6. Goethites from distinct weathering environments reveal varied eU concentrations and ages and lack of positive correlation between (U-Th)/He ages and eU. Noticeably, some of the oldest goethites contain significantly low eU concentrations, while relatively young goethites contain hundreds of ppm eU.

6. Discussion

Weathering of iron-bearing bedrocks favors goethite or hematite precipitation. Once iron complexes enter the weathering solution, environmental parameters such as pH, temperature, salinity, dissolved organic and inorganic ligands, etc. control goethite precipitation rates. Rocks with high iron contents (e.g., BIF, massive sulfides, and ultramafic igneous rocks) tend to produce weathering profiles with large amounts of goethite. These rock types produce some of the purest goethite for dating. Weathering of iron-poor rocks and sediments commonly yield lower abundances of goethite mixed with clay, metal-oxides, and quartz. Availability of U and Th during weathering is also impacted by the concentration of these elements in the bedrock. The (U-Th)/He database clearly shows that goethite may incorporate from very little (<1ppm) to up to 1000's ppm of U and Th (Fig. 4). U-enrichment is favored when oxidizing-acid waters react with U-rich bedrocks at the surface, enrich weathering solutions with soluble U complexes that travel downward into the weathering profile, ultimately precipitating together with iron to form U-rich goethite in the subsurface. High Th concentrations in goethites also generally reflect the Th contents in the bedrock or sediment, but the Th-enrichment mechanism is quite different. Here, weathering fluids carrying Th do not travel far from the source, and Th-rich goethites form locally during recurrent iron metasomatism

of the bedrock and sediment. If this iron metasomatism is long lived, Th-rich goethites may evolve from relatively Th-poor bedrocks such as BIFs and CIDs (Fig. 4).

Paleoclimatic Records in the Global Weathering History

The most complete continental weathering geochronology record is that obtained for parts of cratonic South America (Brazil, Suriname, and Guiana). The record covers a significant area of South America, targeted sites in the continental interior and continental margins, it sampled sites across east-west and north-south traverses, and it investigated a variety of weathering settings (lateritized BIFs, quartzitic karst, lateritized metamorphosed greenstone belts, lateritized carbonatites, lateritized continental sediments, and lateritized Cu-Au deposits) at different elevations. The results for Brazil, Suriname, and Guiana are very similar, showing a progressive increase in the abundance of goethites towards the present, reflecting tropical humid conditions conducive to the recurrent dissolution-reprecipitation of goethite.

Another important observation is that the record of weathering profile development on bedrock shows a longer and more complete weathering history than sites on continental sediments. That history of goethite cementation started at ~70 - 55 Ma in the Carajás Mountains and Quadrilátero Ferrífero (Brazil); ~40 Ma in Catalão (Brazil); ~35 Ma in Suriname and in the Paraná Sedimentary Basin (Brazil); and ~25 Ma in French Guiana and the Espinhaço Range (Brazil). In contrast, the weathering history (goethite cementation) obtained from lateritized unconsolidated sediments is shorter and started from ~10 Ma in the Amazon and southeastern Brazil; from ~17 Ma in northeastern and northern Brazil; and from ~7 Ma in southern Brazil. Detrital goethite-cemented duricrust fragments and pisoliths in these sediments record ages of the weathering profiles from which they were eroded, suggesting effective recycling of iron during weathering-erosion-sedimentation.

The second most complete weathering geochronology record is that obtained for Australia. This record is mainly concentrated in the BIF and CID landscapes of Western Australia, but it contains goethites from Ravensthorpe, Mount Isa, Coochiemudlo Island (Queensland), and South Australia also. The temporal distribution of goethites show increased abundance of young goethite, similar to that observed in South America. But in the Australian case, there is a clear pattern of older goethites concentrated in the continental interior and greater abundance of younger goethites in coastal regions (e.g., Ravensthorpe nickel laterite) (Fig. 6), differently from South America. In the Hamersley Province, for example, there is an abrupt decrease in ages younger than ~5 Ma, suggesting that the interior of Australia transitioned from a wet-warm to dry-warm climate sometime in the late Miocene-Pliocene, decreasing the rate of goethite dissolution-reprecipitation. Another major difference between the Australian and South American records is the significant preservation of ages older than ~ 65 Ma in Australia. Many of these older results are derived from massive goethites eroded from ancient weathering profiles that once covered the BIF ridges and plateaus surrounding paleochannels. The survival of these goethites in the

300   landscape may have resulted from their deposition and burial to shallow depths for most of the Cenozoic combined with a general deficiency in water in Australia as compared with South America. That water deficiency is consistent with the aggradation and preservation of the aggraded rivers in Australia (e.g., CIDs), but their absence in South America, despite very similar landscapes.

305   **A Tectonic Record in the Global Weathering History?**

The weathering records from cratonic South America and Australia suggest a common history of relative tectonic quiescence for the entire Cenozoic. The rocks now undergoing weathering must have been exhumed sometime prior to 80-70 Ma (the oldest weathering ages) and have subsequently remained at the surface, without much vertical movement or reburial-re-
310   exhumation for the entire Cenozoic. This prolonged history of surface exposure is only possible where continental collision, fault reactivation, and other tectonic processes slow to a minimum. A more complete tectonic history written in the weathering record will only emerge when weathering geochronology in South America is extended into the Andes, where tectonism should have played a significant role in weathering profile formation, erosion, and possibly burial and preservation. Similarly, if more widely applied in other continents, particularly North America, Eurasia, and Africa, where
315   contrasting tectonic environments occur within the continental landmasses, it will be possible to discern the role of tectonism in the generation, preservation, or destruction of weathering profiles at a global scale.

7.   Summary

The global database of goethite (U-Th)/He ages and U and Th concentrations shows that a significant effort has been made
320   by different research groups to select, characterize, and date goethite samples preserved in weathering profiles. Goethites from nine weathering environments have been investigated. Goethites from different environments, showing U and Th concentrations varying from < 1ppm to > 1000 ppm have been successfully dated. U and Th enrichment or depletion provide useful complementary information on bedrock compositions and weathering processes. The dataset summarized here clearly shows that the chemical and isotopic compositions of dated goethites record information on changes in
325   environmental conditions through time. The global distribution of goethite (U-Th)/He ages reveals that even though goethite is widely distributed over the surface of the Earth, an immense area of the globe known to contain goethite-bearing weathering profiles has not yet been investigated using the (U-Th)/He method. The database reveals that goethite geochronology applied to weathering studies is still in its infancy, and that paleoenvironmental and paleoclimatic studies will benefit from the broader application of goethite (U-Th)/He geochronology and future methodological developments.

330

Competing interests

The authors declare that they have no conflict of interest.

Author contribution

335

Hevelyn Monteiro: investigation and writing – original draft preparation. Kenneth Farley: funding, writing – review & editing. Paulo Vasconcelos: funding, writing – review & editing.

Acknowledgements

340

This research was supported by NSF grant EAR 1945974 to Kenneth A. Farley.

References

Albuquerque, M. F. S., Horbe, A. M. C., and Danišík, M.: Episodic weathering in Southwestern Amazonia based on (U-Th)/He dating of Fe and Mn lateritic duricrust, Chem. Geol., 553, 119792, 2020.

Allard, T., Gautheron, C., Riffel, S. B., Balan, E., Soares, B. F., Pinna-Jamme, R., Derycke, A., Morin, G., Bueno, G. T., and Nascimento, N.: Combined dating of goethites and kaolinites from ferruginous duricrusts. Deciphering the Late Neogene erosion history of Central Amazonia, Chem. Geol., 479, 136-150, doi: 10.1016/j.chemgeo.2018.01.004, 2018.

Ansart, C., Quantin, C., Calmels, D., Allard, T., Roig, J. Y., Coueffe, R., Heller, B., Pinna-Jamme, R., Nouet, J., Reguer, S., Vantelon, D., and Gautheron, C.: (U-Th)/He Geochronology Constraints on Lateritic Duricrust Formation on the Guiana Shield, Front. Earth. Sci., 10:888993, doi: 10.3389/feart.2022.888993, 2022.

Bassal, F., Heller, B., Roques, J., Balout, H., Tassan-Got, L., Allard, T., Gautheron, C.: Revealing the radiation damage and Al-content impacts on He diffusion in goethite. Chem. Geol. 611, 121118, 2022

Boyle, R. W.: Geochemical prospecting for Thorium and Uranium deposits, Amsterdam: Elsevier, 1982.

Conceição, F. T., Vasconcelos, P. M., Godoy, L. H., Navarro, G. R.B., Montibeller, C. C., and Sardinha, D. S.: Water/rock interactions, chemical weathering and erosion, and supergene enrichment in the Tapira and Catalão I alkaline-carbonatite complexes. Brazil. J. Geochem. Explor. 237, https://doi.org/10.1016/j. gexplo.2022.106999 106999, 2022.

Conceição, F. T., Vasconcelos, P. M., Guillermo R.B. Navarro, G. R. B., and Farley, K. A.: ^{40}Ar/ ^{39}Ar and (U-Th)/He constraints on emplacement, exhumation, and weathering of alkaline-carbonatite complexes in the Alto Paranaíba Igneous Province (APIP), Brazil, Gond. Res., 130, 116-130, doi: 10.1016/j.gr.2024.01.010, 2024.

Danišík, M., Evans, N. J., Ramanaidou, E. R., McDonald, B. J., Mayers, C., and McInnes, B. I. A.: (U–Th)/He chronology of the Robe River channel iron deposits, Hamersley Province, Western Australia, Chem. Geol., 354, 150-162, doi: 10.1016/j.chemgeo.2013.06.012, 2013.

De Campos, D. S., Monteiro, H. S., Vasconcelos, P. M., Farley, K. A., Silva, A. C., and Vidal-Torrado, P.: A new model of bauxitization in quartzitic landscapes: A case study from the Southern Espinhaço Range (Brazil), Earth Surf. Proc. Land., 48, 2788-2807, doi: 10.1002/esp.5660, 2023.

Deng, X.-D., Li, J.-W., and Shuster, D. L.: Late Mio-Pliocene chemical weathering of the Yulong porphyry Cu deposit in the eastern Tibetan Plateau constrained by goethite (U–Th)/He dating: Implication for Asian summer monsoon, E. Planet. Sci. Lett., 472, 289-298, doi: 10.1016/j.epsl.2017.04.043, 2017.

Flowers, R. M., Shuster, D. L., Wernicke, B. P., and K.A. Farley, K. A.: Radiation damage control on apatite (U-Th)/He dates from the Grand Canyon region, Colorado Plateau, *Geology*, 35 (5): 447–450. doi: 10.1130/G23471A.1, 2007.

Golightly, J. P.: Nickeliferous laterite deposits, Econ. Geol., 75th Anniversary Volume, 710-735.

Heim, J. A., Vasconcelos, P. M., Shuster, D. L., Farley, K. A., and Broadbent, G.: Dating paleochannel iron ore by (U-Th)/He analysis of supergene goethite, Hamersley province, Australia, Geology, 34(3), 173-176, oi: 10.1130/G22003.1, 2006.

375   Heller, B., Riffel, S. B., Allard, T., Morin, G., Roig, J. Y., Coueffe, R., Aertgeerts, G., Derycke, A., Ansart, C., Pinna-Jamme, R., Gautheron, C.: Reading the climate signals hidden in bauxite, Geochim. Cosmochim. Acta, 323, 40-73, doi: 10.1016/j.gca.2022.02.017, 2022.

Hofmann, F., Reichenbacher, B., and Farley, K. A.: Evidence for >5 Ma paleo-exposure of an Eocene–Miocene paleosol of the Bohnerz Formation, Switzerland, Earth Planet. Sci. Lett., 465, 168-175, doi: 10.1016/j.epsl.2017.02.042, 2017.

380   Langmuir, D.: Uranium solution-mineral equilibria at low temperature with applications to sedimentary ore deposits, Geochim. Cosmochim. Acta, 42, 547-569, 1978.

Levett, A., Gagen, E. J., Shuster, J., Rintoul, L., Tobin, M., Vongsvivut, J., Bambery, K., Vasconcelos, P. M., and Southam, G.: Evidence of biogeochemical processes in iron duricrust formation, J. South Amer. Earth Sci., 71, 131-142, doi: 10.1016/j.jsames.2016.06.016

385   Levett, A., Vasconcelos, P. M., Gagen, E. J., Rintoul, L., Spier, C., Guagliardo, P., and Southam, G.: Microbial weathering signatures in lateritic ferruginous duricrusts, Earth Palnet. Sci. Lett, 538, 116209, doi: 10.1016/j.epsl.2020.116209, 2020.

Levett, A., Gagen, E. J., Rintoul, L., Guagliardo, P., Diao, H., Vasconcelos, P. M., and Southam, G.: Characterization of iron oxide encrusted microbial fossils, Scient. Reports, 10:9889, doi:10.1038/s41598-020-66830-z, 2020.

Lima, M. G.: A História do Intemperismo na Província Borborema Oriental, Nordeste do Brasil: Implicações
390   Paleoclimáticas e Tectônicas, Ph.D. thesis, Univ. Fed. Rio Grande do Norte, Natal, Brazil, 2008.

Lippolt, H. J., Brander, T., and Mankopf, N. R.: An attempt to determine formation ages of goethites and limonites by (U+Th)-^{4}He dating, Neues Jahr. Mineral.-Monat., 11, 505–528, 1998.

Mabesoone, J. M., Campos-Silva, A., and Buerlen, K.: Estratigrafia e origem do Grupo Barreiras em Pernambuco, Paraíba e Rio Grande do Norte. Rev. Bras. Geoci. 2, 173–188, 1972.

395   Marques, K. P. P., Allard. T., Gautheron, C., Baptiste, B., Pinna-Jamme, R., Morin, G., Delbes, L., and Vidal-Torrado, P.: Supergene phases from ferruginous duricrusts: non-destructive microsampling and mineralogy prior to (U-Th)/He geochronological analysis, Eur. J. Mineral., 35, 383-395, doi: 10.5194/ejm-35-383-2023, 2023.

Massey, M. S., Lezana-Pacheco, J. S., Jones, M. E., Ilton, E. S., Cerrato, J. M., Bargar, J. R., and Fendorf, S.: Competing retention pathways of uranium upon reaction with Fe(II). *Geochimica et Cosmochimica Acta*, **142**, 166-185, 2014.

400

Monteiro, H. S., Vasconcelos, P. M., Farley, K. A., Spier, C. A., and Mello, C. L.: (U–Th)/He geochronology of goethite and the origin and evolution of cangas, Geochim. Cosmochim. Acta, 131, 267-289, doi: 10.1016/j.gca.2014.01.036, 2014.

Monteiro, H. S., Vasconcelos, P. M., and Farley, K. A.: A combined (U-Th)/He and cosmogenic ^{3}He record of landscape armoring by biogeochemical iron cycling. J. Geophys Res.: Earth Surf., 123, 298–323, doi: 10.1002/2017JF004282, 2018a.

405   Monteiro, H. S., Vasconcelos, P. M., Farley, K. A., and Lopes, C. A. M.: Age and evolution of diachronous erosion surfaces in the Amazon: Combining (U-Th)/He and cosmogenic ^{3}He records, Geochim. Cosmochim. Acta, 229, 162-183, doi: 10.1016/j.gca.2011.04.029, 2018b.

Monteiro, H. S., Vasconcelos, P. M., Farley, K. A., Ávila, J. N., Miller, H.B.D., P. Holden, P., Ireland, T. R.: Protocols for in situ measurement of oxygen isotopes in goethite by ion microprobe, Chem. Geol., 533, 119436, doi:
410   10.1016/j.chemgeo.2016.03.033, 2020.

Monteiro, H. S., Vasconcelos, P. M., Farley, K. A., Mello, C. L., and Conceição, F. T.: Long-term vegetation-induced goethite and hematite dissolution-reprecipitation along the Brazilian Atlantic margin, Palaeogeo. Palaeoclim. Palaeoeco., 601, 111137, doi: 10.1016/j.palaeo.2022.111137, 2022.

Reiners, P. W., Chan, M. A., and Evenson, N. S.: (U-Th)/He geochronology and chemical compositions of diagenetic
415   cement, concretions, and fracture-filling oxide minerals in Mesozoic sandstones of the Colorado Plateau, GSA Bull., 126, 1363-1383, doi: 10.1130/B30983.1, 2014.

Riffel, S. B., Vasconcelos, P. M., Carmo, I. O., and Farley, K. A.: Combined ^{40}Ar/^{39}Ar and (U–Th)/He geochronological constraints on long-term landscape evolution of the Second Paraná Plateau and its ruiniform surface features, Paraná, Brazil, Geomorphology, 233, 52-63, doi: 10.1016/j.geomorph.2014.10.041, 2015.

420   Riffel, S. B., Vasconcelos, P. M., Carmo, I. O., and Farley, K. A.: Goethite (U–Th)/He geochronology and precipitation mechanisms during weathering of basalts, Chem. Geol., 446, 18-32, doi: 10.1016/j.chemgeo.2016.03.033, 2016.

Rossetti, D. F., Bezerra, F. H. R., and Dominguez, M. L.: Late Oligocene–Miocene transgressions along the equatorial and eastern margins of Brazil, Earth-Sci. Rev., 123, 87-112, doi: 10.1016/j.earscirev.2013.04.005, 2013.

Shuster, D. L., Vasconcelos, P. M., Farley, K. A., and Heim, J. A.: Weathering geochronology by (U-Th)/He dating of
425   goethite, Geochim. Cosmochim. Acta, 69 (3), 659-673, doi: 10.1016/j.gca.2004.07.028, 2005.

Shuster, D. L., Farley, K. A., Vasconcelos, P. M., Balco, G., S. Monteiro, H. S., Waltenberg, K. M., and Stone, J. O.: Cosmogenic ^{3}He in hematite and goethite from Brazilian "canga" duricrust demonstrates the extreme stability of these surfaces, Earth Planet. Sci. Lett., 329-330, 41-50, doi: 10.1016/j.epsl.2012.02.017, 2012.

Sposito, G.: The chemistry of soils, Oxford University Press, Inc., New York, 329 pages, 2008.

430

Strutt R. J.: The accumulation of helium in geological time III, Proc. Royal Soc. A83, 96 –99, 1910.

Vasconcelos, P. M., Heim, J. A., Farley, K. A., Monteiro, H. S., and Waltenberg, K. M.: $^{40}Ar/ ^{39}Ar$ and (U–Th)/He – 4He/ ^{3}He geochronology of landscape evolution and channel iron deposit genesis at Lynn Peak, Western Australia, Geochim. Cosmochim. Acta, 117, 283-312, doi: 10.1016/j.gca.2013.03.037, 2013.

435   Verhaert, M., Gautheron, C., Dekoninck, A., Vennemann, T., Pinna-Jamme, R., Mouttaqi, A., and Yans, J.: Unravelling the Temporal and Chemical Evolution of a Mineralizing Fluid in Karst-Hosted Deposits: A Record from Goethite in the High Atlas Foreland (Morocco), Minerals, 12, 1151, https://doi.org/10.3390/min12091151, 2022.

Waltenberg, K. M.: Mineral physics and crystal chemistry of minerals suitable for weathering geochronology: implications to $^{40}Ar/^{39}Ar$ and (U-Th)/He geochronology, Ph.D. thesis, The University of Queensland, 2012.

440   Yans, J., Verhaert, M., Gautheron, C., Antoine, P.-O., Moussi, B., Dekoninck, A., Decrée, S., Chaftar, H.-R., Hatira, N., Dupuis, C., Pinna-Jamme, R., and Jamoussi, F.; (U-Th)/He Dating of Supergene Iron (Oxyhydr-)Oxides of the Nefza-Sejnane District (Tunisia): New Insights into Mineralization and Mammalian Biostratigraphy, Minerals, 11, 260, doi: 10.3390/min11030260, 2021.

Yapp, C. J.: Rusty Relics of Earth History: Iron (III) Oxides, Isotopes, and Surficial Environments, Ann. Rev. Earth & 445   Planet. Sci., 29, 165-199, doi: 10.1146/annurev.earth.29.1.165, 2001.

Yapp, C. J. and Shuster, D. L.: Environmental memory and a possible seasonal bias in the stable isotope composition of (U–Th)/He-dated goethite from the Canadian Arctic, Geochim. Cosmochim. Acta, 75, 4194-4215, doi: 10.1016/j.gca.2011.04.029, 2011.

Yapp, C. J. and Shuster, D. L.: D/H of late Miocene meteoric waters in Western Australia: Paleoenvironmental conditions 450   inferred from the δD of (U-Th)/He-dated CID goethite, Geochim. Cosmochim. Acta, 213, 110-136, doi: 10.1016/j.gca.2017.06.036, 2017.